

Depth dependency of indentation hardness during solid-state phase transition of shape memory alloys

Abbas Amini,¹ Wenyi Yan,² and Qingping Sun^{1,a)}

¹Department of Mechanical Engineering, Hong Kong University of Science and Technology, Kowloon, Hong Kong

²Department of Mechanical and Aerospace Engineering, Monash University, Victoria 3800 Melbourne, Australia

(Received 13 April 2011; accepted 2 June 2011; published online 11 July 2011)

We conducted the measurement of the hardness-depth relationship of NiTi shape memory alloy with a sharp Berkovich indenter. Different from most ductile metals, NiTi reacts to the mechanical load of indentation through phase transition underneath the indentation tip. We found that the hardness decreases rapidly with the increase of the indentation depth and eventually approaches a constant. To understand the depth dependency, we performed energy analysis involving the bulk and the interface energies of the transformation zone. We derived the hardness-depth relationship which well explains the experimental results. The finding is useful in hardness measurement of materials involving solid-state phase transitions. © 2011 American Institute of Physics.

[doi:10.1063/1.3603933]

The phenomenon of the increase in the hardness with the decrease of the indentation depth in many metallic materials is well known and has been reported in literatures.¹⁻⁶ The understanding and modeling of such hardness-depth relationship or size effect was mainly based on the dislocation theory and the resulting continuum strain gradient plasticity theory.^{1,2}

Different from most ductile metallic materials where plasticity is the dominant deformation mechanism, shape memory alloys (SMAs) react to the mechanical load of indentation through phase transition. SMAs are increasingly used as candidate materials for micro- and nano-scale devices. In these very small length scales, the hardness of the material has attracted great interest and become an important factor in evaluating the mechanical performance and reliability such as wear and friction behavior. The instrumented indentation technique is frequently used to measure the hardness of the SMAs at nano- to micro-scales.⁷⁻¹⁵ However, the depth dependency in the measured hardness of NiTi has not been examined so far. In this letter, we conduct indentation hardness test on NiTi SMA to examine its depth dependency and perform a simple analysis to understand the observed phenomenon.

Commercial 500 μm thick NiTi polycrystalline sheets were purchased from Memory Applications Inc., USA. The nominal alloy composition was Ni-56.4% and Ti-43.6% (wt. %). The size of the grain was in the range of 50-100 nm as observed by transmission electron microscopy (TEM). The sheet was cut (5 mm \times 5 mm) into pieces and polished by a series of silicon carbide and aluminum oxide sand papers with a minimum grain diameter of 0.05 μm , until the average surface roughness was less than 6 nm as checked by a 3D surface profiler (SPM NT3300, Wyko, USA). The material is initially in austenite phase, and martensite phase is induced by the in-

dentation stress and remain after unloading, exhibiting shape memory effect (SME) as shown in Fig. 1. Therefore, the stress-strain relationship of the material consists of the elastic deformation of austenite, phase transition stage, and elastic loading and unloading of martensite phase.¹⁶ All nanoindentations were conducted in a quasi-static mode by Wrexham (USA) at two temperatures ($T = 23^\circ\text{C}$ and $T = 70^\circ\text{C}$) using a Berkovich tip of radius ~ 50 nm with a constant force rate of 1 mN/s. Before carrying out the indentation tests, the Wrexham instrument was carefully calibrated by following standard procedures. The range of the maximum loads was from 1 mN to 450 mN. To avoid the effect of the tip radius on the results, only those indentation data with depths over 150 nm were considered.

Figure 2 shows the indentation curves with different maximum indentation loads. All the curves have features of plasticity-like response with residual depths, which are mainly due to the retained phase transition strain after unloading. It is understood that plastic deformation due to

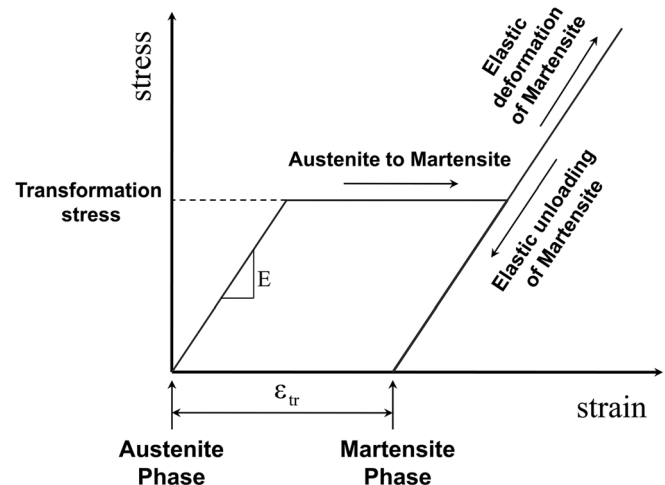


FIG. 1. Schematic stress-strain curve for SMA material.

^{a)} Author to whom correspondence should be addressed. Electronic mail: meqpsun@ust.hk. Tel.: (+852)23588655. FAX: (+852)23581543.

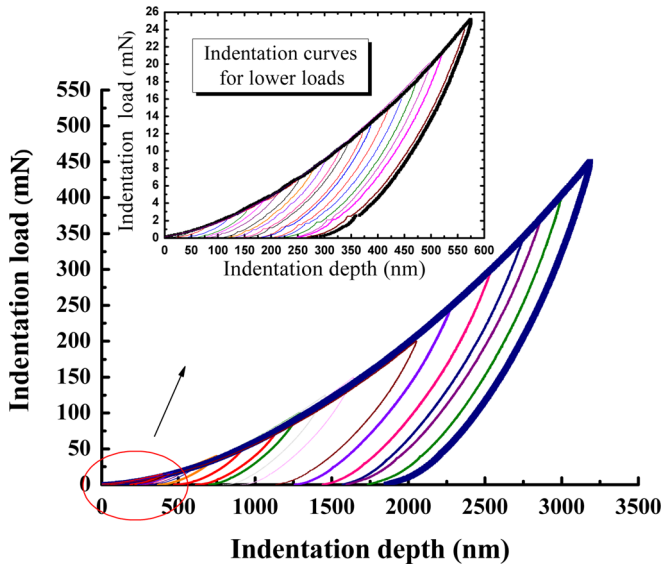


FIG. 2. (Color online) Indentation curves at $T = 23^\circ\text{C}$.

dislocation can occur due to the sharp indenter tip. However, the plastic zone is expected to be much smaller than the phase transition zone, because the plastic yielding stress of martensite phase (~ 1200 MPa) is much higher than the phase transition stress (~ 300 MPa).^{7,10} This has been confirmed from the numerical results of the finite element simulations of SMA indentation.^{17–19} Therefore, the response in Fig. 2 is mainly associated with and determined by the phase transition process instead of the plastic deformation. The hardness is extracted from the indentation force-depth curves (Fig. 2) using the Oliver-Pharr method,²⁰ and we plot the hardness-maximum depth data as shown in Fig. 3. It is seen that the measured hardness, instead of being a material constant, exhibits a significant depth dependency, i.e., the smaller the depth, the larger the hardness of the material. By increasing the indentation depth, the hardness decreases from ~ 11 GPa to the saturated amount of nearly 2 GPa. The data in two different temperatures have similar trend.

To understand the above results, consider an indentation process as shown in Fig. 4. The phase transition zone increases with the load. The variation of the system's total free energy includes the mechanical energy of external force,

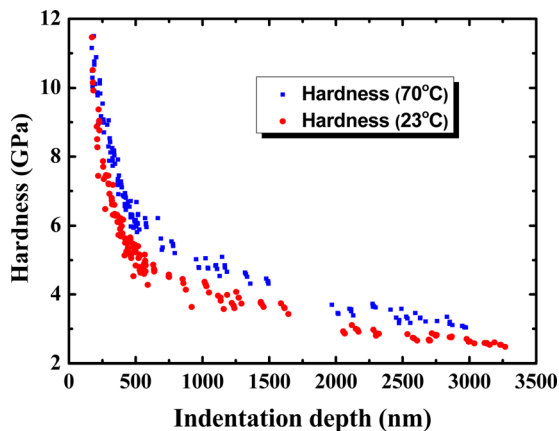


FIG. 3. (Color online) Hardness versus indentation depth at two different temperatures.

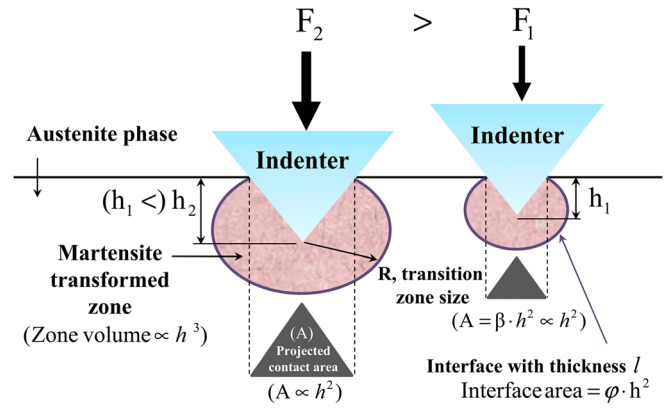


FIG. 4. (Color online) Schematic transformation zone, interface area, and projected contact area under two different forces.

the interface energy of the transition zone, the bulk chemical free energy, and the elastic misfit strain energy. Treating the loading process with phase transition as a monotonic nonlinear elastic deformation and using the energy minimization principal, the indentation depth-hardness relationship can be derived in following.

The total Gibbs free energy (G) of the system under given force can be expressed as

$$\begin{aligned} G(T, F, h) &= U_{\text{external}} + U_{\text{interface}} + U_{\text{bulk}} \\ &= -F \cdot h + U_{\text{interface}} + U_{\text{bulk}}. \end{aligned} \quad (1)$$

In Eq. (1), U_{external} is the potential energy of the external indentation force (F), h is the indentation depth, U_{bulk} is the change in bulk energy (misfit strain energy and chemical free energy) of the transformed volume (from the austenite to martensite), and $U_{\text{interface}}$ is the interface energy of the martensite zone. For sharp indentation using Berkovich indenters, it is well known that the martensite zone grows in a geometrically self-similar way, and the zone size (R) is proportional to the indentation depth (h).²¹ The surface area of the zone scales with h^2 and the volume of the zone scales with h^3 .²¹ We can write the following expressions for $U_{\text{interface}}$ and U_{bulk} :

$$U_{\text{interface}} = \varphi \cdot \gamma_{\text{front}} \cdot h^2 = \varphi \cdot (k \cdot l \cdot E \cdot \varepsilon_{\text{tr}}^2) \cdot h^2, \quad (2)$$

$$U_{\text{bulk}} = \underbrace{\varphi_1 \cdot E \cdot \varepsilon_{\text{tr}}^2 \cdot h^3}_{\text{elastic strain energy}} + \underbrace{\varphi_2 \cdot \Delta G(T) \cdot h^3}_{\text{chemical free energy change}}. \quad (3)$$

In $U_{\text{interface}}$, φ is the non-dimensional shape factor in calculating the interface area, γ_{front} is the interface energy density (energy per unit area, assuming isotropic interface energy) of the martensite zone, and γ_{front} can be expressed as $\gamma_{\text{front}} = k \cdot l \cdot E \cdot \varepsilon_{\text{tr}}^2$, where E is Young's modulus of the material, ε_{tr} is the characteristic transformation strain, k is a small coefficient and l is the characteristic thickness of the interface. In U_{bulk} , φ_1 and φ_2 are the non-dimensional zone shape factors used in calculating the bulk elastic misfit strain energy and the chemical free energy changes, $\Delta G(T)$ is the change in chemical free energy density (per unit volume).

The condition for the system to be in equilibrium requires

$$\frac{\partial G}{\partial h} = 0. \quad (4)$$

Substituting Eqs. (1)–(3) into (4), we obtain the expression of F as

$$F = 2\varphi \cdot k \cdot l \cdot E \cdot \varepsilon_{tr}^2 \cdot h + 3\varphi_1 \cdot E \cdot \varepsilon_{tr}^2 \cdot h^2 + 3\varphi_2 \cdot \Delta G(T) \cdot h^2 \quad (5)$$

Using Eq. (5) and the projected contact area $A = \beta h^2$ with $\beta = 24.56$ for the Berkovich tip, we have the hardness as

$$H = H(h, T) = \frac{F}{A} = \beta_1 \left(\frac{l}{h} \right) + \beta_2, \quad (6)$$

where $\beta_1 = \frac{2}{24.56} \varphi \cdot k \cdot E \cdot \varepsilon_{tr}^2$ and $\beta_2 = \frac{3}{24.56} (\varphi_1 \cdot E \cdot \varepsilon_{tr}^2 + \varphi_2 \cdot \Delta G(T))$. Eq. (6) shows that the depth dependence of the hardness is dictated by the ratio $\frac{l}{h}$, i.e., the smaller the depth, the higher the hardness of the material. When the depth is large enough, i.e., $\frac{l}{h} \rightarrow 0$, the measured hardness is degenerated into the constant β_2 which is determined by the characteristic bulk properties ($E \cdot \varepsilon_{tr}^2$ and $\Delta G(T)$) of the material and the domain shape (φ_1, φ_2), as shown in the following

$$H|_{\frac{l}{h} \rightarrow 0} = H_0 = \beta_2 = \frac{3}{24.56} (\varphi_1 \cdot E \cdot \varepsilon_{tr}^2 + \varphi_2 \cdot \Delta G(T)). \quad (7)$$

It is seen that H_0 depends on the temperature through $\Delta G(T)$. Alternatively, we can express the hardness as

$$\tilde{H} = \frac{H}{H_0} = 1 + \frac{\beta_1 l}{\beta_2} \left(\frac{1}{h} \right) = 1 + \alpha \left(\frac{1}{h} \right), \quad (8)$$

where $\alpha (= \frac{\beta_1 l}{\beta_2})$ is the lump coefficient which depends on the tip geometry, bulk, and interface properties of the material. α can be obtained by curve-fitting.

From the above analysis, it is seen that the observed depth dependence of the measured transformation hardness originates from the involvement of both bulk and interface energy terms in the phase transition process under mechanical force. The contribution of both terms to the measured hardness can be expressed by the ratio l/h of the two characteristic length scales. In another word, for very small indentation depth (l/h is very large), surface energy is dominant in the energy of the system; while for very large indentation depth ($l/h \rightarrow 0$), the contribution of surface energy is ignorable in the total energy of the system. According to this rationale, the test data are plotted in Fig. 5. It is seen that the derived scaling law of Eq. (6) well captures the data of the observed depth dependency. We should notice that all the hardness calculation and analysis are based on the limited information from the measured load-depth curves; direct experimental verifications on the characteristic length scale of the zone size and interface thickness are still needed.

In summary, we found a strong depth dependency in the measured transformation hardness of the NiTi SMA at small indentation depths. The hardness increases significantly with the decrease in the indentation depth. By a simple energy analysis it is revealed that such size effect in the measured hardness is attributed to the competition of bulk and interface

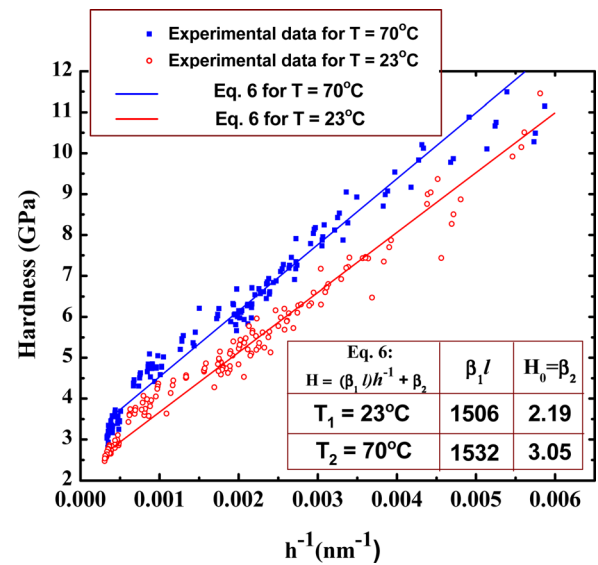


FIG. 5. (Color online) Hardness versus reciprocal of indentation depth.

energy terms in the phase transition process. Different from most ductile metals for which the depth dependence follows an inverse square-root power law scaling,² the phase transition hardness follows an inverse depth-dependence scaling (i.e., a reciprocal relationship with the depth). The theoretical rationale is supported by the experimental results.

Partial financial support from the Hong Kong Research Grants Council under a CERG grant (No. 620109) is gratefully acknowledged.

¹M. S. De-Guzman, G. Neubauber, P. Flinn, and W. D. Nix, *Mater. Res. Soc. Symp. Proc.* **308**, 613 (1993).

²W. D. Nix and H. Gao, *J. Mech. Phys. Solids* **46**, 411 (1998).

³Z. Xue, Y. Huang, K. C. Hwang, and M. Li, *J. Eng. Mater. Technol.* **124**, 371 (2002).

⁴W. Ni, Y. T. Cheng, and D. S. Grummon, *Appl. Phys. Lett.* **82**, 2811 (2003).

⁵K. Gall, K. Juntunen, H. J. Maier, H. Sehitoglu, and Y. I. Chumlyakov, *Acta Mater.* **49**, 3205 (2001).

⁶A. Amini, Y. He, and Q. P. Sun, *Mater. Lett.* **65**, 464 (2011).

⁷L. Qian, Q. P. Sun, and X. Xiao, *Wear* **260**(4-5), 509 (2006).

⁸W. Yan, Q. P. Sun, X.-Q. Feng, and L. Qian, *Int. J. Solids Struct.* **44**, 1 (2007).

⁹W. Yan, Q. P. Sun, and H.-Y. Liu, *Mater. Sci. Eng., A* **425**, 278 (2006).

¹⁰L. M. Qian, X. D. Xiao, Q. P. Sun, and T. X. Yu, *Appl. Phys. Lett.* **84**, 1076 (2004).

¹¹Y. J. He and Q. P. Sun, *Int. J. Solids Struct.* **46**, 4242 (2009).

¹²Y. J. He and Q. P. Sun, *Int. J. Mech. Sci.* **52**, 198 (2010).

¹³Q. P. Sun and Y. J. He, *Int. J. Solids Struct.* **45**, 3868 (2008).

¹⁴A. A. Elmustafa and D. S. Stone, *J. Mech. Phys. Solids* **51**, 357 (2003).

¹⁵B. Xu, W. M. Huang, Y. T. Pei, Z. G. Chen, A. Kraft, R. Reuben, J. T. M. De Hosson, and Y. Q. Fu, *Eur. Polym. J.* **45**, 1904 (2009).

¹⁶D. A. Porter and K. E. Easterling, *Phase Transformations in Metals and Alloys* (Chapman & Hall, London, 1992).

¹⁷G. Kang and W. Yan, *Appl. Phys. Lett.* **94**, 261906 (2009).

¹⁸G. Kang and W. Yan, *Philos. Mag.* **90**, 599 (2010).

¹⁹Y. Zhang, Y.-T. Cheng, and D. S. Grummon, *J. Appl. Phys.* **101**, 053507 (2007).

²⁰W. C. Oliver and G. M. Pharr, *J. Mater. Res.* **7**, 1564 (1992).

²¹R. Hill, *The Mathematical Theory of Plasticity* (Oxford University Press, New York, 1950).